CHEMISTRY
A EUROPEAN JOURNAL

DOI: 10.1002/chem.200700858

An Ionically Driven Molecular IMPLICATION Gate Operating in Fluorescence Mode

Knut Rurack,*[a] Christian Trieflinger,[b] Anton Koval'chuck,[a] and Jörg Daub*[b]

Abstract: An asymmetrically core-extended boron–dipyrromethene (BDP) dye was equipped with two electron-donating macrocyclic binding units with different metal ion preferences to operate as an ionically driven molecular IMPLICATION gate. A Na^+-responsive tetraoxa-aza crown ether (R^2) was integrated into the extended π system of the BDP chromophore to trigger strong intramolecular charge transfer (ICT_2) fluorescence and guarantee cation-induced spectral shifts in absorption. A dithia-oxa-aza crown (R^1) that responds to Ag^+ was attached to the *meso* position of BDP in an electronically decoupled fashion to independently control a second ICT_1 process of a quenching nature. The bifunctional molecule is designed in such a way that in the absence of both inputs, ICT_1 does not compete with ICT_2 and a high fluorescence output is obtained ($In_A = In_B = 0 \rightarrow Out = 1$). Accordingly, binding of only Ag^+ at R^1 ($In_A = 1$, $In_B = 0$) as well as complexation of both receptors ($In_A = In_B = 1$) also yields $Out = 1$. Only for the case in which Na^+ is bound at R^2 and R^1 is in its free state does quenching occur, which is the distinguishing characteristic for the $In_A = 0$ and $In_B = 1 \rightarrow Out = 0$ state that is required for a logic IMPLICATION gate and Boolean operations such as IF-THEN or NOT.

Keywords: charge transfer · dyes/pigments · fluorescence · logic gates · molecular devices

Introduction

Since the first reports on molecular logic gates,[1] the development of molecules that are capable of performing Boolean operations has received increasing attention.[2,3] The concept of molecular logic is fuelled by the long-term goal of molecular computation,[4] but some recent examples have shown that, in the short term, the implementation of Boolean operations at the molecular scale can also improve the performance of methods and stimulate new advances in the fields of chemical sensing, diagnostics, and functional biochemistry.[5–8] Molecular logic gates operate at nanometric dimensions[9] and are in most cases designed to deliver an optical output when fed with chemical or optical inputs, which potentially uses all of the benefits of light and luminescence as a media for communication.

Today, a variety of molecular logic gates have been reported.[2,3] Sophisticated examples are able to process more than two inputs[7,10] or can even execute simple arithmetic calculations.[5,8] Initial integrated arrays of molecular logic gates[11] and practical applications, such as molecular computational identification,[6] have also recently been reported. However, when examining the table of Boolean operations,[12] it is apparent that small molecule and biomolecule-based logic gates have mainly been developed for the commutative operations AND/NAND (G_1/G_{14}), OR/NOR (G_7/G_8), and XOR/EQU (G_6/G_9) as well as for two of the four non-commutative gates, the exclusion or INHIBIT gates G_2 and G_4 (Table 1).[13] With respect to IMPLICATION gates (G_{11} and G_{13}), to the best of our knowledge, only one report of a molecular logic gate has been published so far.[14] However, IMPLICATION operations in which one input implies the other, that is, if input A is equal to one then input B has to be equal to zero, are important because they are equivalent to the IF-THEN operation and the NOT operation.[15] Aside from AND and OR, NOT is one of the three key Boolean operations in database searching and information

[a] Dr. K. Rurack, A. Koval'chuck
Div. I.5 "Bioanalytik", Bundesanstalt für Materialforschung und -prüfung (BAM)
Richard Willstätter Strasse 11, 12489 Berlin (Germany)
Fax: (+49) 30-8104-5005
E-mail: knut.rurack@bam.de

[b] Dr. C. Trieflinger, Prof. J. Daub
Institut für Organische Chemie, Universität Regensburg
Universitätsstrasse 31, 93053 Regensburg (Germany)
Fax: (+49) 941-943-4984
E-mail: joerg.daub@chemie.uni-regensburg.de

Supporting information for this article is available on the WWW under http://www.chemeurj.org/ or from the author.

Table 1. Selected commutative and non-commutative Boolean operations.[a] For further details on all 16 gates,[b] see Table S1 in the Supporting Information.

Gate No.[a,b]	A = 0 B = 0[c]	A = 0 B = 1[c]	A = 1 B = 0[c]	A = 1 B = 1[c]	Logic gate[d]	Ref.[e]
G_1	0	0	0	1	AND(†)	[44]
G_2	0	0	1	0	INHIBIT	[45]
G_4	0	1	0	0	INHIBIT	[45]
G_6	0	1	1	0	XOR(§)	[46]
G_7	0	1	1	1	OR(#)	[47]
G_8	1	0	0	0	NOR(#)	[48]
G_9	1	0	0	1	EQU(§)	[17,49]
G_{11}	1	0	1	1	IMPLY	[14]
G_{13}	1	1	0	1	IMPLY	[14]
G_{14}	1	1	1	0	NAND(†)	[50]

[a] The notation used in this article was adopted from ref. [43]. [b] Six of the sixteen operations are rather trivial in terms of molecular design and fluorescence output, see the Supporting Information. [c] Output pattern for Input combinations. [d] Abbreviations in accordance with ref. [43]. These abbreviations are used in most articles on molecular logic gates. Symbols in brackets relate commutative operations. IMPLY stands for IMPLICATION. [e] Two representative references of molecular logic gates performing the respective operation have been chosen from the recent literature.

retrieval.[16] On the basis that logic gates with fluorescence readout are particularly attractive and that the first example reported by de Silva and McClenaghan was achieved by using changes in transmittance,[14] we present here the design of and proof-of-principle for an ionically driven molecular IMPLICATION gate that operates through fluorescence.

Abstract in German: *Ein am Kern unsymmetrisch verlängerter Bordipyrromethen-(BDP) Farbstoff wurde mit zwei Elektronen schiebenden makrozyklischen Bindungseinheiten, die sich in ihren Metallionenpräferenzen unterscheiden, versehen, um als molekulares IMPLICATION-Gatter zu fungieren. Um eine starke intramolekulare Ladungstransfer- (intramolecular charge transfer, ICT_2) Fluoreszenz zu generieren und Kationen induzierte spektrale Verschiebungen in Absorption zu garantieren, wurde ein auf Na^+ ansprechender Tetraoxa-aza-Kronenether R^2 in das verlängerte π-System des BDP-Chromophors integriert. Ein Dithia-oxa-aza-Kronenether R^1, welcher auf Ag^+ anspricht, wurde an der meso-Position des BDP-Körpers in einer elektronisch entkoppelten Art und Weise eingeführt, um unabhängig von ICT_2 einen zweiten, die Fluoreszenz löschenden ICT_1 kontrollieren zu können. Das bifunktionelle Molekül wurde so konstruiert, dass ICT_1 in der Abwesenheit beider Eingabeparameter nicht mit ICT_2 konkurrieren kann und ein intensives Fluoreszenzsignal ausgegeben wird ($In_A = In_B = 0 \rightarrow Out = 1$). Dementsprechend führt die alleinige Bindung von Ag^+ an R^1 ($In_A = 1$, $In_B = 0$) sowie die Komplexierung beider Rezeptoren ($In_A = In_B = 1$) ebenfalls zu $Out = 1$. Nur wenn Na^+ an R^2 gebunden wird und R^1 in freiem Zustand vorliegt, erfolgt Fluoreszenzlöschung. Letzteres zeichnet den charakteristischen Zustand $In_A = 0$, $In_B = 1 \rightarrow Out = 0$ aus, der für das logische IMPLICATION-Gatter und Boolesche Operationen wie IF-THEN oder NOT benötigt wird.*

Results and Discussion

Design considerations and synthesis: Most molecular logic gates reported in the literature to date display changes in fluorescence as output (Out) signals and generally utilize photoinduced electron transfer (PET) or intramolecular charge transfer (ICT) as the addressable processes.[2,3] As the majority of these systems are AND, OR, XOR, or INHIBIT gates, in which Out equals zero in the absence of both inputs (In), the challenge was to create a molecule that is fluorescent (Out = 1) when $In_A = In_B = 0$ and is only quenched in the presence of one input alone, as required for IMPLICATION (Table 1). Because IMPLICATION gates are non-commutative and cannot be expressed by the negation of one of the other fifteen gates, conventional design employing, for instance, two PET processes was ruled out. Systems based on two PET processes are usually quenched in the free state and the presence of one and/or the other input interrupts PET and leads to enhanced emission, which often shows AND or OR behavior.[2] Furthermore, when two ICT processes are coupled in a fully conjugated donor–acceptor[17] or donor–acceptor–donor system,[18] commutative XOR, EQU, or NAND gates result. Instead, we implemented two ICT processes in our target structure **1** (Scheme 1), but chose an electronically decoupled architecture so that one of the ICT processes formally represents a PET process through a "virtual" or zero spacer.[19] The dye scaffold that seemed most suitable to us for realization of our aim was the boron–dipyrromethene (BDP) chromophore that has versatile functionalisation chemistry and is suited to multiple switching of fluorescence by different inputs.[20] The synthesis of **1** followed a procedure that was previously employed for the preparation of **3**,[21] that is, treating **2**[22] with 4-(1,4,7,10-tetraoxa-13-azacyclopentadecan-13-yl)benzaldehyde[23] in the presence of acetic acid, piperidine, and molecular sieves in toluene at reflux.

Realization of $In_A = In_B = 0 \rightarrow Out\ 1 = 1$: The two π-conjugated units in 8-aryl-substituted BDPs are perpendicularly oriented when the BDP core has two methyl groups in the 1 and 7 positions ($\theta \approx 90°$, Scheme 1). The π systems of the dipyrromethene unit and the aromatic group at the 8-position are electronically decoupled. As the 8-phenyl group has neither an electron donor nor acceptor character, it has virtually no influence on the optical properties of the BDP chromophore (Figure 1). Compound **4** shows the characteristic intense BDP fluorescence at around 510 nm in solvents of any polarity with, for example, $\Phi_f(\mathbf{4}) = 0.60$ in MeCN.[24] If

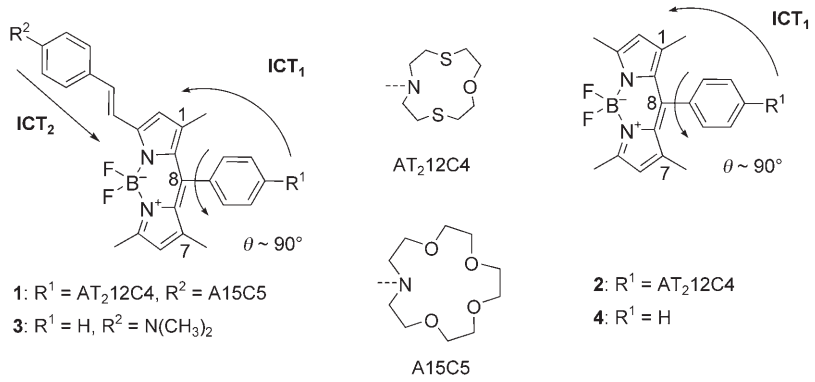

Scheme 1. Chemical structures of molecular logic gate **1** and model compounds **2**–**4**. ICT_1 and ICT_2 denote addressable processes.

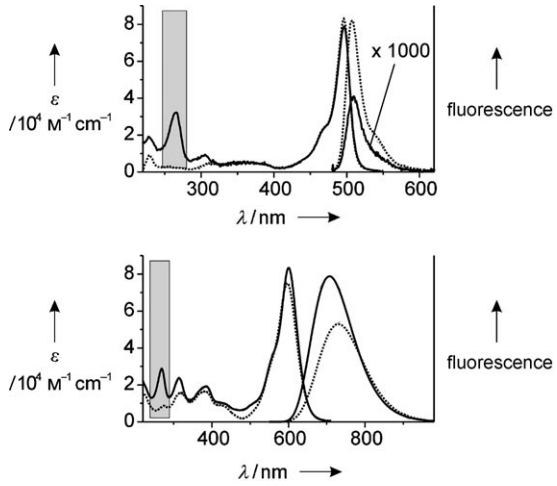

Figure 1. Absorption and fluorescence spectra of **2** (solid line, top) and **4** (dotted line, top), and **1** (solid line, bottom) and **3** (dotted line, bottom) in acetonitrile at 298 K ($c_{\mathbf{1}\text{-}\mathbf{4}}=2$ μM). The fluorescence spectrum of **2** was magnified for a better comparison. The light grey bars indicate the region of the lowest-energy transition localized on the anilino group in the 8-position of **1** and **2**.

an electron-donating group, such as a crown aniline, is introduced to the 8-position, both units are still decoupled in the ground state and the absorption spectrum of **2** is a linear combination of the bands of the subunits with maxima at $\lambda=265$ (aniline) and 497 nm (BDP). After excitation in polar solvents however, an excited-state ICT process (ICT_1 in Scheme 1) is activated. As ICT_1 involves decoupled moieties, it has a largely forbidden nature and quenches the fluorescence ($\Phi_f(\mathbf{2})\approx10^{-4}$ for **2** in MeCN) while having virtually no effect on the spectral position of the emission band (Figure 1, top).[22]

In contrast, if an amino group is introduced through a styryl extension to the BDP core as in **3**, a π-conjugated, planar ICT chromophore with redshifted absorption at around 600 nm, is obtained in which the amino and BDP groups act as donor and acceptor (Figure 1).[21] As the styryl–BDP chromophore remains planar in the excited state, ICT_2 is highly allowed and **3** is a brightly red-emitting dye with $\Phi_f(\mathbf{3})=0.13$ in MeCN. Important for the design of **1** is now the fact that the step from **4** to **3** raises the energy of the HOMO localized on the styryl–BDP fragment sufficiently[25] so that exchange of an 8-phenyl for an 8-anilino group (step from **3** to **1**) does not activate the quenching ICT_1 process, therefore, **1** is also brightly red fluorescent (Table 2, Figure 1). As the A15C5 unit at R^2 in **1** is a weaker donor than the $N(CH_3)_2$ group in **3**, the emission of **1** is blueshifted by 25 nm. This shift reduces the influence of internal conversion according to the energy-gap law and leads to a higher Φ_f of **1** than **3**.[21] In conclusion, for **1**, $In_A=In_B=0$ results in $Out_{\mathbf{1}}=1$ (Table 3).

Table 2. Spectroscopic data of **1** in the absence and presence of the two inputs Ag^+ (In_A) and Na^+ (In_B) in acetonitrile at 298 K.

Species	ε_{265} [M^{-1} cm^{-1}]	λ_{abs}(BDP) [nm]	λ_{em} [nm]	Φ_f
1	28500	600	707	0.18
1–Ag^+	14600	604	717	0.21
Na^+–**1**	27200	572	703	0.04
Na^+–**1**–Ag^+	15000	574	707	0.19

Table 3. Truth table of operations for **1** (IMPLY stands for IMPLICATION).

In_A Ag^+	In_B Na^+	$Out_{\mathbf{1}}$ Φ_f	$Out_{\mathbf{2}}$ ε_{265}	$Out_{\mathbf{3}}$ λ_{abs}^{600}	$Out_{\mathbf{4}}$ (λ_{abs}^{265}+λ_{abs}^{600})
0	0	1	1	1	1
1	0	1	0	1	1
0	1	0	1	0	1
1	1	1	0	0	0
		IMPLY	INV A	INV B	NAND

Figure 2 illustrates the charge-transfer features with the aid of gas-phase calculations of **1**–**4** and the protonated species of **1**.[26] When comparing the energy level diagrams of **1**–**4**, it is apparent that the ICT_1 process from a molecular orbital localized on the 8-substituent to the LUMO localized on the BDP can only successfully compete with the BDP-centered transition in highly polar environments for **2**.

Performance in the presence of inputs: The other In/Out combinations can be rationalized as follows: Binding of a cationic input (Ag^+) at decoupled R^1 engages the lone electron pair of the anilino nitrogen, thus diminishing the absorption band at 265 nm (see ε_{265} entry for **1**–Ag^+ in Table 2 and inset of Figure 3), and reduces the strength of the 8-donor. The latter has no effect on the fluorescence because unbound R^1 is already a strong donor and is unable to

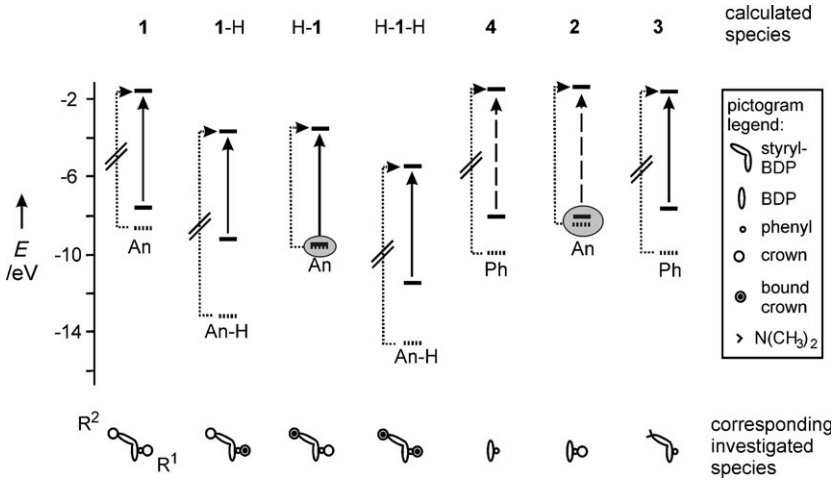

Figure 2. Schematic representation of energy levels of the frontier molecular orbitals localized on the styryl–BDP or BDP (solid line) and the highest lying occupied MOs localized on the 8-aryl moiety (dotted line; An = aniline, An–H = protonated aniline, Ph = phenyl) as calculated for **1**–**4** and protonated derivatives (denoted "H") as model structures for the complexes (see pictograms) in the gas phase. Solid arrows: ICT_2, dashed arrows: BDP-localized (LE), and dotted arrows: ICT_1 transitions. In polar solvents, ICT_1 with a higher dipole moment than ICT_2 and a much higher dipole moment than LE can be sufficiently stabilized only for H–**1** and **2** (gray circles) to induce quenching.

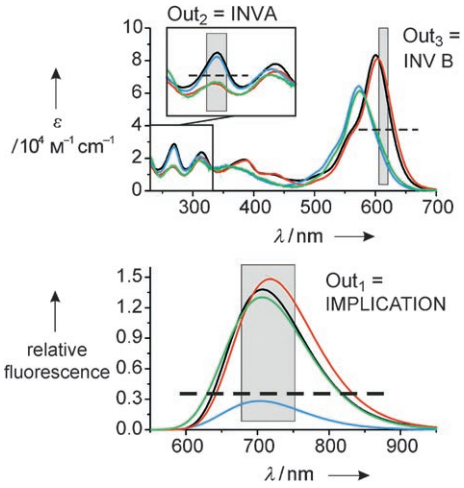

Figure 3. Absorption (top) and fluorescence (bottom) spectra of **1** (black), **1**–Ag^+ (red), Na^+–**1** (blue), and Na^+–**1**–Ag^+ (green) in acetonitrile at 298 K ($c_1 = 2$ μM, $c_{Ag} = 0.5$ mM, $c_{Na} = 20$ mM). The inset shows the enlarged high-energy region of the absorption spectra. Horizontal lines mark the thresholds for readout "0" versus "1", gray bars mark the spectral windows for optimum readout.

quench the fluorescence through the ICT_1 pathway. Binding of Ag^+ further lowers the energy level of the molecular orbital (MO) localized on the 8-group with respect to the frontier MOs (cf. **1** vs. **1**–H, Figure 2) so that $In_A = 1$ and $In_B = 0$ yields $Out_1 = 1$ (Figure 3, Table 3). Ag^+ (0.5 mM) was chosen for In_A because it binds selectively to $AT_2$12C4 in acetonitrile at that concentration and not to A15C5.[27,28] At that concentration full complexation is also guaranteed. With regards to ICT_2 and the installation of the single specific $Out_1 = 0$, it was also important to use a cation as In_B because binding of a cation at donor R^2 reduces ICT_2. The latter effect shifts the electronic features in such a way that quenching by ICT_1 from unbound R^1 is now activated (**1** vs. H–**1** in Figure 2, Figure 3). Na^+ (20 mM), which has a high preference for A15C5, was chosen to be In_B.[29] As in the case of Ag^+, the chosen concentration guarantees full complexation. The entries for Na^+–**1** in Tables 2 and 3 show that when $In_A = 0$ and $In_B = 1$ the fluorescence is indeed quenched and $Out_1 = 0$.

The results for $In_A = In_B = 1$ are then straightforward. When Ag^+ is added to a solution of Na^+–**1**, activated ICT_1 is again interrupted (cf. H–**1** vs. H–**1**–H in Figure 2) and fluorescence is restored ($Out_1 = 1$). The same is found when Na^+ is added to **1**–Ag^+ (**1**–H to H–**1**–H, Figure 2), that is, a highly fluorescent species remains highly fluorescent. Control experiments revealed that in agreement with the coordination chemistry of mixed heteroatom macrocycles[30] and studies on other ICT probes that contain either the A15C5 or the $AT_2$12C4 crown,[22,31,32] all of the complexation reactions discussed herein are reversible.[33] The use of a metal ion responsive R^2 was not only important to trigger the quenching process, but also to guarantee that all of the emission bands appear in the same spectral region. If protons were used as inputs then the combination of PET and ICT in a single molecule would again yield only commutative operations, such as XOR/EQU[34] or OR/NOR.[35] However, when employing metal ion receptors one can profit from the fact that in styryl dyes with ICT processes, such as ICT_2 in **1**, metal ion binding leads to strong blueshifts in absorption yet minor shifts in emission owing to excited-state de-coordination.[31,32] The latter avoids covalent bond formation, for example, by protonation, and hence, undesirable blueshifts in both absorption and emission. Therefore, Na^+–**1** and Na^+–**1**–Ag^+ only show hypsochromically shifted absorption bands, but emission bands that largely overlap with those of **1** (Figure 3), which enables readout at one emission wavelength.

Conclusion

In summary, a first molecular IMPLICATION gate based on a specific fluorescence-quenching mechanism was developed by integrating two decoupled, yet communicating, ICT processes in a small molecule and two metal ion inputs. The quenched state (Out = 0) for $In_A = 0$ and $In_B = 1$, which distinguishes an IMPLICATION gate was achieved by electron

density control through site-specific metal ion complexation. When considering all of the different outputs as shown in Table 3, **1** is not only an IMPLICATION gate, but also delivers the INVerted input pattern through specific absorption signals (whenever Ag^+/Na^+ is present the aniline/BDP band is diminished) and serves as a NAND gate through the combined absorption response. After having demonstrated the proof-of-principle, current work is now aimed at addressing the issues of ion concentration, because it would be desirable to use similar concentrations for both inputs, and operation in aqueous media.

Experimental Section

General: All solvents and chemicals were of reagent grade quality, obtained commercially, and used without further purification. Melting points were recorded on a Reichert Thermovar micro melting apparatus and are not corrected. ^{1}H NMR spectra were measured by using an Avance 300 spectrometer. Mass spectra were recorded by using Varian CH-5 and Finigan MAT 95 instruments. IR spectra were obtained by using a Biorad FTS 155 spectrometer with KBr disks. All solvents employed for spectroscopic measurements were of UV-spectroscopic grade and purchased from Aldrich. Metal perchlorates purchased from Aldrich were of highest purity available and dried as described previously.[32]

Synthesis of 1: Compound 2 (0.020 g, 0.04 mmol),[22] *N*-A15C5-benzaldehyde (0.015 g, 0.04 mmol),[23] acetic acid (0.15 mL), piperidine (0.18 mL), and a small amount of molecular sieves (3–4 Å) in toluene (5 mL) were heated at reflux for 48 h. After cooling, separation by five chromatographic runs on silica gel by using dichloromethane/acetonitrile (5:3) as the eluent, and preparative HPLC **1** was obtained as a blue solid (0.006 mg, 0.007 mmol, 16%). M.p. 178–180 °C; ^{1}H NMR (400 MHz, $CDCl_3$, TMS): $\delta = 7.49$–7.46 (m, 3H; aryl, CH=CH), 7.20–7.14 (m, 1H; CH=CH), 7.06–7.03 (m, 2H; aryl), 6.73–6.58 (m, 5H; aryl, pyrrole−H), 5.95 (s, 1H; pyrrole−H), 3.82–3.54 (m, 28H; CH_2), 2.96–2.82 (m, 8H; CH_2), 2.57 (s, 3H; CH_3), 1.53 (s, 3H; CH_3), 1.50 ppm (s, 3H; CH_3); FTIR (KBr): 2967, 2935, 2857, 1656, 1594, 1543, 1529, 1496, 1384, 1298, 1182, 1120, 986 cm^{-1}; MS (EI, 70 eV): m/z: (%): 834 (100) [M^+]; HRMS (EI, 70 eV): m/z: calcd: 834.3841; found: 834.3836;.[36]

Optical spectroscopy: Absorption and fluorescence measurements were carried out in acetonitrile by using a Cary 5000 UV/Vis-near-infrared spectrophotometer and a Spectronics Instrument 8100 spectrofluorometer. For all measurements, the temperature was kept constant at 298 ± 1 K. Only dilute solutions with an absorbance of less than 0.1 at the absorption maximum were used. Fluorescence experiments were performed with a 90° standard geometry, with polarizers set at 54.7° for emission and 0° for excitation. The fluorescence quantum yields (Φ_f) of **1** were determined relative to cresyl violet in methanol ($\Phi_f = 0.54 \pm 0.03$)[37] and rhodamine 101 in ethanol ($\Phi_f = 1.00 \pm 0.02$).[38] All of the fluorescence spectra presented herein were spectrally corrected as described in ref. [39] The uncertainties of measurement were determined to be ±5% (for $\Phi_f > 0.2$) and ±10% (for $0.2 > \Phi_f$).

Quantum chemical calculations: Geometry optimizations were performed by employing the semiempirical AM1 method (gradient < 0.01; AMPAC V6.55, Semichem).[40] Transition energies were calculated on the basis of the corresponding ground-state geometries and 1SCF calculations with a singly excited CI approach including 129 configurations by the methods AM1 (Ampac V6.55, Semichem) and ZINDO/S.[41] Owing to the low quality of the parameterization of the metal cations in the program, the various protonated species of **1** that represent the extreme points of analyte binding were modeled and analyzed theoretically. As binding of the metal ion to the nitrogen, the only heteroatom of the receptor that is integrated into the chromophoric π system, is the single binding event that is decisive for the spectroscopic response, the other heteroatoms in the crown, which presumably coordinate to the metal ion, have no relevance for the trends of shifts to be expected in the chromophore. Moreover, calculations of protonated species are known to yield reliable approximations of the metal ion complexes for illustrative purposes.[25,42] The values in Figure 2 are thus only a schematic representation of trends that are also to be expected for the metal ion complexes.

Acknowledgements

Financial support by the DFG (Deutsche Forschungsgemeinschaft), the Studienstiftung des Deutschen Volkes and Bundesanstalt für Materialforschung und -prüfung (BAM) PhD Program is gratefully acknowledged. We thank Dr. Michael Büschel for synthetic help. This work is part of the Graduate College "Sensory Photoreceptors in Natural and Artificial Systems", Universität Regensburg (DFG, GRK 640).

[1] A. P. de Silva, H. Q. N. Gunaratne, C. P. McCoy, *Nature* **1993**, *364*, 42–44; P. Ball, *Nature* **2000**, *406*, 118–120.
[2] A. P. de Silva, Y. Leydet, C. Lincheneau, N. D. McClenaghan, *J. Phys. Condens. Matter* **2006**, *18*, S1847-S1872.
[3] V. Balzani, A. Credi, M. Venturi, *ChemPhysChem* **2003**, *4*, 49–59; F. M. Raymo, *Adv. Mater.* **2002**, *14*, 401–414.
[4] A. P. de Silva, *Nat. Mater.* **2005**, *4*, 15–16; K. P. Zauner, *Crit. Rev. Solid State Mater. Sci.* **2005**, *30*, 33–69.
[5] D. Margulies, G. Melman, A. Shanzer, *Nat. Mater.* **2005**, *4*, 768–771.
[6] A. P. de Silva, M. P. James, B. O. F. McKinney, D. A. Pears, S. M. Weir, *Nat. Mater.* **2006**, *5*, 787–790.
[7] H. Lederman, J. Macdonald, D. Stefanovic, M. N. Stojanovic, *Biochemistry* **2006**, *45*, 1194–1199.
[8] R. Baron, O. Lioubashevski, E. Katz, T. Niazov, I. Willner, *Angew. Chem.* **2006**, *118*, 1602–1606; *Angew. Chem. Int. Ed.* **2006**, *45*, 1572–1576.
[9] R. F. Service, *Science* **2001**, *293*, 782–785.
[10] D. C. Magri, G. J. Brown, G. D. McClean, A. P. de Silva, *J. Am. Chem. Soc.* **2006**, *128*, 4950–4951.
[11] J. Macdonald, Y. Li, M. Sutovic, H. Lederman, K. Pendri, W. Lu, B. L. Andrews, D. Stefanovic, M. N. Stojanovic, *Nano Lett.* **2006**, *6*, 2598–2603.
[12] The interested reader can find more detailed information on the internationally accepted and approved Table of Boolean Operations for two inputs provided by the InterNational Committee for Information Technology Standards (INCITS) on its website at http://www.incits.org/tc_home/k5htm/andfig04.gif.
[13] Six of the sixteen operations are rather trivial in terms of molecular design and fluorescence output, see Table S1 in the Supporting Information.
[14] A. P. de Silva, N. D. McClenaghan, *Chem. Eur. J.* **2002**, *8*, 4935–4945.
[15] Here the Boolean NOT operator for two inputs is meant and not the single input/single output NOT gate or inverter, see for instance ref. [49].
[16] For typical examples, see the help pages for the STN database provided by CAS at: http://www.cas.org/training/stncommands/operators.html#P33_294; the National Center of Biotechnology Information at the NIH's National Library of Medicine at: http://www.ncbi.nlm.nih.gov/books/bv.fcgi?rid=helpentrez.section.Entrez-Help.Boolean_Operators; or the University Libraries, University at Albany, SUNY at: http://www.internettutorials.net/boolean.html; for an example of using three Boolean operators for data mining, see: I. N. Kouris, C. H. Makris, A. K. Tsakalidis, *Data Knowl. Eng.* **2005**, *52*, 353–383.
[17] A. P. de Silva, N. D. McClenaghan, *J. Am. Chem. Soc.* **2000**, *122*, 3965–3966.
[18] K. Rurack, A. Koval'chuck, J. L. Bricks, J. L. Slominskii, *J. Am. Chem. Soc.* **2001**, *123*, 6205–6206.
[19] K. Rurack, U. Resch-Genger, *Chem. Soc. Rev.* **2002**, *31*, 116–127.

[20] C. Trieflinger, K. Rurack, J. Daub, *Angew. Chem.* **2005**, *117*, 2328–2331; *Angew. Chem. Int. Ed.* **2005**, *44*, 2288–2291; C. Trieflinger, H. Röhr, K. Rurack, J. Daub, *Angew. Chem.* **2005**, *117*, 7104–7107; *Angew. Chem. Int. Ed.* **2005**, *44*, 6943–6947; H. Röhr, C. Trieflinger, K. Rurack, J. Daub, *Chem. Eur. J.* **2006**, *12*, 689–700.

[21] K. Rurack, M. Kollmannsberger, J. Daub, *Angew. Chem.* **2001**, *113*, 396–399; *Angew. Chem. Int. Ed.* **2001**, *40*, 385–387.

[22] J. L. Bricks, A. Kovalchuk, C. Trieflinger, M. Nofz, M. Büschel, A. I. Tolmachev, J. Daub, K. Rurack, *J. Am. Chem. Soc.* **2005**, *127*, 13522–13529.

[23] J. P. Dix, F. Vögtle, *Chem. Ber.* **1980**, *113*, 457–470.

[24] M. Kollmannsberger, K. Rurack, U. Resch-Genger, J. Daub, *J. Phys. Chem. A* **1998**, *102*, 10211–10220.

[25] Y.-H. Yu, A. B. Descalzo, Z. Shen, H. Röhr, Q. Liu, Y.-W. Wang, M. Spieles, Y.-Z. Li, K. Rurack, X.-Z. You, *Chem. Asian J.* **2006**, *1*, 176–187.

[26] See the Experimental Section for details. Unfortunately attempts to measure the redox potentials did not provide exploitable results for the Ag^+ complexes, most likely owing to limitations in solubility and possible side reactions. Thus, we relied on the quantum chemical results for further illustration of the mechanism of operation.

[27] Fe^{3+} and Cu^{2+} ions that are much better bound by **2** than Ag^+ readily oxidize **1** in MeCN so that Ag^+ was employed here (see ref. [22]).

[28] Ag^+ ions do not bind to A15C5 at these concentrations, see ref. [18].

[29] Na^+ ions do not bind to $AT_2$12C4 at these rather high concentrations, see ref. [22] This is most likely owing to the fact that the two sulfur atoms neighboring the nitrogen and separating nitrogen and oxygen atom of the crown are not coordinating to Na^+ (for a detailed discussion of the influence of heteroatom nature and topology on the coordination chemistry of crowned bifunctional molecular probes, see ref. [51]). It is also well-known from studies of many fluoroionophores and reference dyes that the anilino nitrogen atom alone is unable to coordinate to Na^+ even at a very high excess in acetonitrile, see ref. [32].

[30] R. M. Izatt, K. Pawlak, J. S. Bradshaw, R. L. Bruening, *Chem. Rev.* **1991**, *91*, 1721–2085; A. P. de Silva, H. Q. N. Gunaratne, T. Gunnlaugsson, A. J. M. Huxley, C. P. McCoy, J. T. Rademacher, T. E. Rice, *Chem. Rev.* **1997**, *97*, 1515–1566.

[31] R. Mathevet, G. Jonusauskas, C. Rulliére, J. F. Létard, R. Lapouyade, *J. Phys. Chem.* **1995**, *99*, 15709–15713.

[32] K. Rurack, J. L. Bricks, G. Reck, R. Radeglia, U. Resch-Genger, *J. Phys. Chem. A* **2000**, *104*, 3087–3109.

[33] Owing to the fact that at the concentrations employed herein complexation is site specific[28,29] and based on many studies of crowned fluoroionophores that identified the formation of well-defined species at Na^+ concentrations such as 20 mM (e.g., S. Fery-Forgues, M.-T. Le Bris, J.-P. Guetté, B. Valeur, *J. Phys. Chem.* **1988**, *92*, 6233–6237; J. Bourson, B. Valeur, *J. Phys. Chem.* **1989**, *93*, 3871–3876; S. Das, K. G. Thomas, K. J. Thomas, P. V. Kamat, M. V. George, *J. Phys. Chem.* **1994**, *98*, 9291–9296; S. Das, K. G. Thomas, K. J. Thomas, M. V. George, I. Bedja, P. V. Kamat, *Anal. Proc.* **1995**, *32*, 213–215; K. Rurack, J. L. Bricks, B. Schulz, M. Maus, G. Reck, U. Resch-Genger, *J. Phys. Chem. A* **2000**, *104*, 6171–6188;[24]), unspecific effects owing to high ionic strengths can be ruled out and well-defined species, as indicated by Na^+–**1**, Ag^+–**1** and Na^+–**1**–Ag^+, are responsible for the distinct and reproducible spectroscopic responses found here. Moreover, mixed coordination that yields multiple species would also entail more complicated spectroscopic responses, see, for example, refs. [32,51].

[34] A. Coskun, E. Deniz, E. U. Akkaya, *Org. Lett.* **2005**, *7*, 5187–5189.

[35] K. Rurack, J. L. Bricks, *Arkivoc* **2001**, 31–40.

[36] With regards to coupling constants, we refrained from a first-order analysis because the protons of the two crowns were not well resolved in the spectrum and the aromatic protons showed only slight differences in the chemical shifts. The structure and purity of **1** is nonetheless confirmed by the high-resolution MS data and the UV/Vis spectra, that is, molar absorption coefficients of $83\,300\,M^{-1}\,cm^{-1}$ in acetonitrile for the styryl-extended BDP chromophore and $28\,500\,M^{-1}\,cm^{-1}$ for the aniline chromophore (Table 2, Figure 1).

[37] D. Magde, J. H. Brannon, T. L. Cremers, J. Olmsted III, *J. Phys. Chem.* **1979**, *83*, 696–699.

[38] D. F. Eaton, *Pure Appl. Chem.* **1988**, *60*, 1107–1114.

[39] J. Hollandt, R. D. Taubert, J. Seidel, U. Resch-Genger, A. Gugg-Helminger, D. Pfeifer, C. Monte, W. Pilz, *J. Fluoresc.* **2005**, *15*, 301–313; U. Resch-Genger, D. Pfeifer, C. Monte, W. Pilz, A. Hoffmann, M. Spieles, K. Rurack, J. Hollandt, D. Taubert, B. Schönenberger, P. Nording, *J. Fluoresc.* **2005**, *15*, 315–336.

[40] M. J. S. Dewar, E. G. Zoebisch, E. F. Healy, J. J. P. Stewart, *J. Am. Chem. Soc.* **1985**, *107*, 3902–3909.

[41] M. M. Karelson, M. C. Zerner, *J. Phys. Chem.* **1992**, *96*, 6949–6957.

[42] K. Rurack, M. Sczepan, M. Spieles, U. Resch-Genger, W. Rettig, *Chem. Phys. Lett.* **2000**, *320*, 87–94.

[43] P. Burger, *Digital Design, A Practical Course*; J. Wiley & Sons, New York, **1988**.

[44] S. Uchiyama, N. Kawai, A. P. de Silva, K. Iwai, *J. Am. Chem. Soc.* **2004**, *126*, 3032–3033; J. Andréasson, Y. Terazono, B. Albinsson, T. A. Moore, A. L. Moore, D. Gust, *Angew. Chem.* **2005**, *117*, 7763–7766; *Angew. Chem. Int. Ed.* **2005**, *44*, 7591–7594.

[45] D.-H. Qu, F.-Y. Ji, Q.-C. Wang, H. Tian, *Adv. Mater.* **2006**, *18*, 2035–2038; T. Gunnlaugsson, D. A. Mac Dónail, D. Parker, *Chem. Commun.* **2000**, 93–94.

[46] L. F. O. Furtado, A. D. P. Alexiou, L. Goncalves, H. E. Toma, K. Araki, *Angew. Chem.* **2006**, *118*, 3215–3218; *Angew. Chem. Int. Ed.* **2006**, *45*, 3143–3146; D. Margulies, G. Melman, C. E. Felder, R. Arad-Yellin, A. Shanzer, *J. Am. Chem. Soc.* **2004**, *126*, 15400–15401.

[47] R. J. Amir, M. Popkov, R. A. Lerner, C. F. Barbas III, D. Shabat, *Angew. Chem.* **2005**, *117*, 4452–4455; *Angew. Chem. Int. Ed.* **2005**, *44*, 4378–4381; P. Singh, S. Kumar, *New J. Chem.* **2006**, *30*, 1553–1556.

[48] S. H. Lee, J. Y. Kim, S. K. Kim, J. H. Lee, J. S. Kim, *Tetrahedron* **2004**, *60*, 5171–5176; Y. Shiraishi, Y. Tokitoh, T. Hirai, *Chem. Commun.* **2005**, 5316–5318.

[49] Y. Tang, F. He, S. Wang, Y. Li, D. Zhu, G. C. Bazan, *Adv. Mater.* **2006**, *18*, 2105–2110.

[50] A. Saghatelian, N. H. Völcker, K. M. Guckian, V. S. Y. Lin, M. R. Ghadiri, *J. Am. Chem. Soc.* **2003**, *125*, 346–347; H. T. Baytekin, E. U. Akkaya, *Org. Lett.* **2000**, *2*, 1725–1727.

[51] B. García-Acosta, R. Martínez-Máñez, F. Sancenón, J. Soto, K. Rurack, M. Spieles, E. García-Breijo, L. Gil, *Inorg. Chem.* **2007**, *46*, 3123–3135.

Received: June 4, 2007
Published online: August 20, 2007

